

LETTER OPEN ACCESS

# Host Competitive Asymmetries Accelerate Viral Evolution in a Microbe–Virus Coevolutionary System

Armun Liaghaf<sup>1,2</sup> | Martin Guillemet<sup>3,4</sup> | Rachel Whitaker<sup>5,6</sup> | Sylvain Gandon<sup>4</sup>  | Mercedes Pascual<sup>2,7,8</sup> 

<sup>1</sup>Department of Ecology and Evolution, University of Chicago, Chicago, Illinois, USA | <sup>2</sup>Department of Biology, New York University, New York, New York, USA | <sup>3</sup>Institute for Integrative Biology, ETH Zürich, Zürich, Switzerland | <sup>4</sup>CEFE, CNRS, Université de Montpellier, EPHE, IRD, Montpellier, France | <sup>5</sup>Carl R. Woese Institute for Genomic Biology, University of Illinois at Urbana-Champaign, Urbana, Illinois, USA | <sup>6</sup>Department of Microbiology, University of Illinois at Urbana-Champaign, Urbana, IL, USA | <sup>7</sup>Department of Environmental Studies, New York University, New York, NY, USA | <sup>8</sup>Santa Fe Institute, Santa Fe, New Mexico, USA

**Correspondence:** Mercedes Pascual ([mercedes.pascual@nyu.edu](mailto:mercedes.pascual@nyu.edu))

**Received:** 11 February 2025 | **Revised:** 14 May 2025 | **Accepted:** 19 May 2025

**Editor:** Pejman Rohani

**Funding:** This work was supported by the Gordon and Betty Moore Foundation, GBMF 9195, funded by the National Science Foundation DBI Biology Integration Institutes Programme, Award Number 2022049.

**Keywords:** microbe–virus coevolution | multiple modes of selection | negative frequency-dependent selection | predator–prey | viral persistence

## ABSTRACT

Microbial host populations evolve traits conferring specific resistance to viral predators via various defence mechanisms, while viruses reciprocally evolve traits to evade these defences. Such coevolutionary dynamics often involve diversification promoted by negative frequency-dependent selection. However, microbial traits conferring competitive asymmetries can induce directional selection, opposing diversification. Despite extensive research on microbe–virus coevolution, the combined effect of both host trait types and associated selection remains unclear. Using a CRISPR-mediated coevolutionary system, we examine how the co-occurrence of both trait types impacts viral evolution and persistence, previously shown to be transient and nonstationary in computational models. A stochastic model incorporating host competitive asymmetries via variation of intrinsic growth rates reveals that competitively advantaged host clades generate the majority of immune diversity. Greater asymmetries extend viral extinction times, accelerate viral adaptation locally in time and augment long-term local adaptation. These findings align with previous experiments and provide further insights into long-term coevolutionary dynamics.

## 1 | Introduction

Pangenomic analyses are increasingly revealing the breadth of both inter- and intraspecific diversity that co-occur in natural microbial populations and communities. These analyses pinpoint conserved genes that code for traits mediating core cellular functions like transcription and translation, and more variable genes that code for accessory traits like those conferring antibiotic and viral resistance and metabolic capabilities to name a few (Mira et al. 2010; Medini et al. 2005; Rouli et al. 2015; Hyun et al. 2022). The effects of trait variation

established by different and co-occurring genomic regions on the coevolution of microbes and their natural enemies remain a largely unexplored avenue. Of particular relevance to strain diversity are the co-occurring trait axes that respectively confer specificity in ecological interactions between natural enemies and their resources, and thus induce density and/or frequency-dependent selection, and variation in intrinsic rates and therefore demography, leading to positive selection. Modern coexistence theory (MCT) establishes the conditions required by these two co-occurring trait axes to give rise to co-existence or exclusion in a purely density-dependent ecological

This is an open access article under the terms of the [Creative Commons Attribution-NonCommercial-NoDerivs License](https://creativecommons.org/licenses/by-nc-nd/4.0/), which permits use and distribution in any medium, provided the original work is properly cited, the use is non-commercial and no modifications or adaptations are made.

© 2025 The Author(s). *Ecology Letters* published by John Wiley & Sons Ltd.

context (Chesson 2000). Namely, differences in the first trait axis contribute to coexistence and the emergence of niches, opposing the effect of differences in the second trait axis which reduce diversity. The absence of differences in either kind of trait corresponds to equivalent species in the sense of ecological neutral theory. The MCT framework has been recently extended to competition of two related strains in the population dynamics of infectious diseases (Park et al. 2024).

Nevertheless, consideration of explicit evolution in this trait framework has been limited, despite its relevance to microbes given timescales similar to those of ecological dynamics. Work by Good et al. provides an exception with a mathematical model of microbial consumers and their resources, where mutations introduce novel trait alleles (Good et al. 2018). Importantly, the expectations of these previous frameworks do not necessarily apply to high-dimensional trait spaces with large variation, or to nontrivial network structures of ecological interactions (who interacts with whom) (Song et al. 2019; Barabás et al. 2018). Moreover, despite advances in addressing coexistence at equilibrium in high-dimensional ecological systems (Doebeli and Ispolatov 2010; Allesina and Tang 2012; May 1972), the joint effect of the above co-occurring trait axes also remains poorly understood, especially in systems with comparable timescales of demography and trait innovation. Here, we address this question with a stochastic model for the coevolutionary host-pathogen dynamics of a microbe-lytic virus system with CRISPR-Cas immune memory.

The CRISPR-Cas system is an immune system found in the accessory genome of many microbial species. This adaptive immune system operates by integrating DNA fragments of infecting viruses, known as ‘protospacers’, into the microbial host’s genome as ‘spacers’ (Van Der Oost et al. 2014). The CRISPR spacer arrays encoded in the host’s genome thus act as a multilocus, sequence-specific immune memory of past infections (Van Der Oost et al. 2014). The presence of a spacer-protospacer match in a subsequent host-virus encounter confers protection against viral infection and lysis. High host and viral strain diversity and nontrivial network interaction structures (‘who infects who’, ‘who is protected from whom’) emerge in the transient temporal dynamics, partly enabled by a large combinatoric trait space from viral repertoire and host memory array sizes, and viral protospacer mutations and host spacer acquisitions. This is in contrast to the simple, one-to-one, infection network structures observed in the ‘kill-the-winner’ model proposed for antiviral defence mechanisms such as surface resistance and restriction modification systems (Thingstad 2000; Winter et al. 2010).

Previous studies of CRISPR-mediated coevolution have largely focused on the emergent and cumulative host immune diversity and structure promoted by negative frequency-dependent selection. In particular, theoretical studies have revealed transient coexistence of host and pathogen, with an alternation of dynamics between periods when hosts establish control of viral proliferation and those of major viral epidemics with associated rapid host-virus co-diversification. In these transient dynamics, the ultimate fate of the pathogen is extinction. The role of (proto-)spacer diversity and network structure in transitions between these phases has also been extensively

addressed (Childs et al. 2014, 2012; van Houte et al. 2016; Morley et al. 2017; Chabas et al. 2018; Pilosof et al. 2020; Liaghat et al. 2024).

Alongside CRISPR-induced immune memory, competitive abilities for resources can also vary among host strains. Recent short-term coevolutionary experiments by Guillemet et al. consider a population of *Streptococcus thermophilus* with both CRISPR immune diversity and competitive asymmetries, supporting ‘royal family’ dynamics of host immune strains previously introduced by Guillemet et al. (2022) and Breitbart et al. (2018). Namely, after a large viral epidemic the majority of descendant immune strains that fix belong to lineages that are competitively dominant. These competitive asymmetries can induce directional selection among host strains and thus losses of immune diversity, counteracting the diversity-maintaining force of negative frequency-dependent selection previously mentioned. The effect and role of these two co-occurring and opposing modes of selection on CRISPR-mediated coevolutionary dynamics remain unexplored in theoretical studies to date.

Some previous models have addressed the combined effects of host resistance and competitive differences, for example the classic ‘kill-the-winner’ (KTW) model and its more recent derivatives (Thingstad 2000; Winter et al. 2010; Xue and Goldenfeld 2017; Marantos et al. 2022), which emphasise viral predation as the mechanism maintaining the coexistence of hosts with competitive differences. In more general studies of host-pathogen systems, multilocus gene-for-gene models have been used to examine the dynamics emerging from fitness costs associated with the possession of multiple resistance alleles (Frank 1993; Thrall and Burdon 2003; Sasaki 2000). Current theory has yet to consider the coevolutionary consequences of host competitive differences in light of the heritable adaptive immunity characteristic of the CRISPR-Cas system.

In this study, we examine the co-occurrence of two key host trait axes: CRISPR-induced memory and competitive asymmetries (see Figure 1 for a schematic diagram). The former trait yields negative frequency-dependent selection, promoting immune diversity among hosts to escape infection by viral populations, allowing the organisation of niches (see Pilosof et al. (2017) for examples of associated network signatures). In contrast, the latter trait leads to directional selection, which constrains the maintenance of such diversity. We investigate the impact of these counteracting selective pressures on viral evolution and persistence. To this end, we extend a previous computational branching process model of CRISPR-mediated microbe-lytic virus coevolution to include differences in host competitive abilities (Liaghat et al. 2024). We specifically assume that competitive asymmetries between host strains are manifest as differences in intrinsic growth rates encoded by an underlying trait locus. The intensity of selection acting on this trait determines the breadth of intrinsic growth-rate variation. Total fitness of a host strain is then a function of both its immune memory and intrinsic growth rate. With numerical simulations, we investigate dynamical outcomes of diversity for both host immunity and intrinsic growth rates, systematically examine the effect of increasing host selection intensity on viral persistence and associated metrics and compare viral adaptation measures for extreme selection regimes. We also discuss correspondences to the

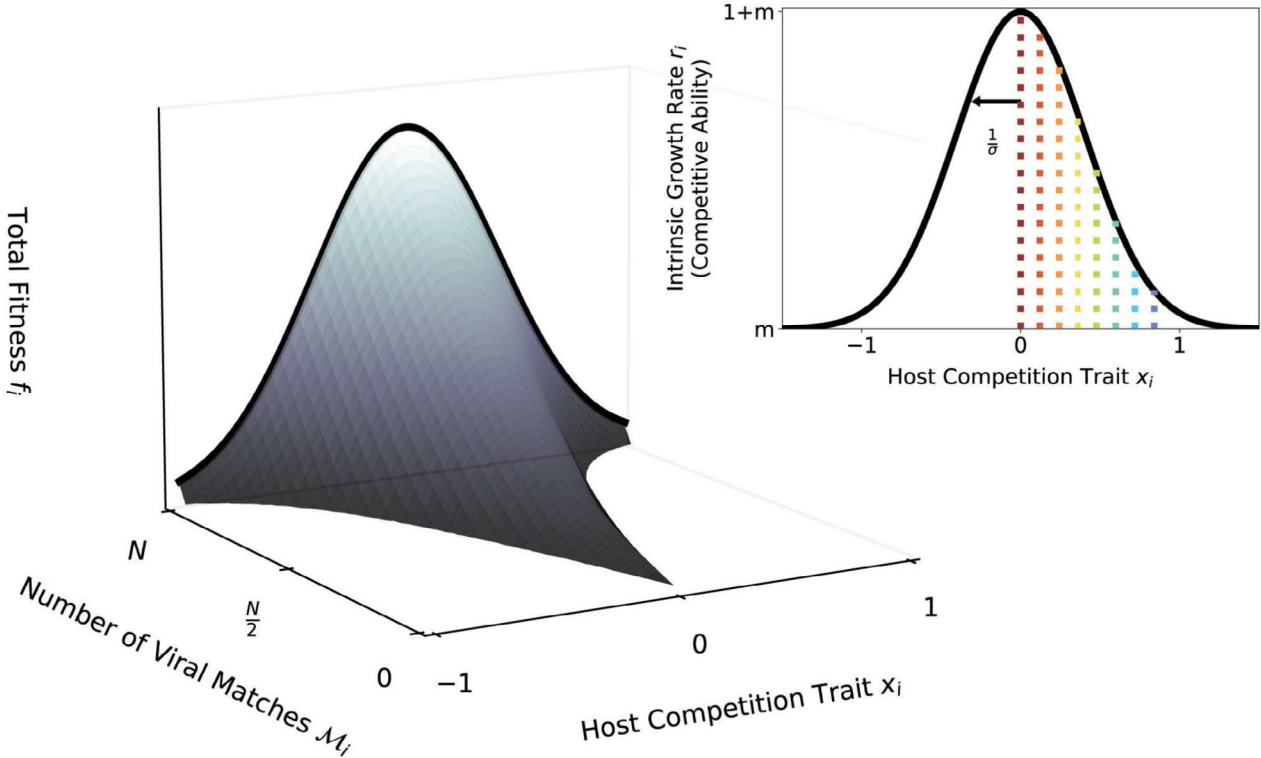


**FIGURE 1** | Diagram of host fitness as a function of two trait axes of a microbial host strain. Negative frequency-dependent and directional selection emerge from the variation of such traits, respectively. The axis labelled as host-competition trait has an absolute effect on fitness further depicted in the inset. Namely, the intrinsic growth rates in our model are a continuous Gaussian function of  $x_i$ , given by  $r_i = e^{-\sigma x_i^2} + m$ , where  $m$  is the washout rate and  $\sigma$  is the associated selection intensity. The associated variation in intrinsic growth rates represents underlying host competitive asymmetries. The other axis represents a component of fitness that depends on the viral diversity and associated frequencies, and is therefore time variable. It monotonically increases with the number of viral matches of the host at a given time. When a host strain matches all viral strains (i.e.,  $M_i = N$ ), or in the absence of viruses, the fitness of a host is dominated by competitive asymmetries leading to directional selection (i.e., competitive exclusion). As  $M_i$  decreases, the host strain becomes susceptible to a larger frequency of the viral population, thus reducing total fitness. The functional form of such decline in the  $M_i$  axis depends on the structure and frequencies of viral diversity, which changes in time. Note that in an extension of the model, the host-competition trait randomly mutates upon a spacer acquisition event (with a probability  $\mu_s$ ). The coloured vertical lines in the inset correspond to the host-competition traits and associated intrinsic growth rates selected for the example dynamics in Figure 2 and our general analyses.

empirical observations of Guillemet et al. (Guillemet et al. 2022) on ‘royal family’ dynamics.

## 2 | Methods

### 2.1 | Model

We extend a stochastic model of CRISPR-mediated microbe and lytic virus coevolution, a multi-type branching process implemented computationally with a Gillespie algorithm. Events are implemented as an inhomogeneous Poisson process, where time is continuous and event times are exponentially distributed with corresponding rates. Microbial hosts in our model replicate at a rate  $r$ , and ‘washout’ at a rate  $m$ . To model asymmetries in competitive abilities, we introduce variation among the intrinsic growth rates  $r$  of the initialized microbial hosts. We attribute a trait locus to every host strain which encodes an intrinsic growth rate. This locus takes an allelic value  $x$  from the interval  $[-1, 1]$  which encodes for an intrinsic growth rate  $r$  defined by the continuous Gaussian function  $r = \exp(-\sigma x^2) + m$ , where  $\sigma$  represents the intensity of selection. As selection intensifies, the half-maximum width of the fitness function shortens, causing

the higher fitness values to be represented by fewer trait values around the origin. As selection weakens due to the lack of competitive asymmetries,  $\sigma \rightarrow 0$ , the fitness function approaches uniformity (i.e., neutrality). Figure 1 depicts an example of the map between competition trait alleles and intrinsic growth rates for the eight host strains used to initialize simulations of our model. We note that the intrinsic growth rate  $r$  can be derived by a standard time-scale separation in consumer-resource dynamics, where resource dynamics are assumed to equilibrate much faster than those of consumers (see O’Dwyer (2018) for the conditions required for this approximation in an ODE context). Hence, the function and associated trait locus we utilise to define growth here is meant to abstract a composite of underlying traits related to consumption preferences, and associated uptake and metabolic rates.

Moreover, a viral strain naturally decays at a rate  $d$  and is defined by a repertoire with a fixed number of loci  $g$  that carry discrete traits often referred to as *protospacers* (Van Der Oost et al. 2014). Upon adsorption that occurs at a rate  $\varphi$  per particle, a microbe utilises its CRISPR-Cas immune system to evade lysis with a probability  $q$ , such that one of the  $g$  protospacers of a viral strain is randomly selected then integrated as a so-called

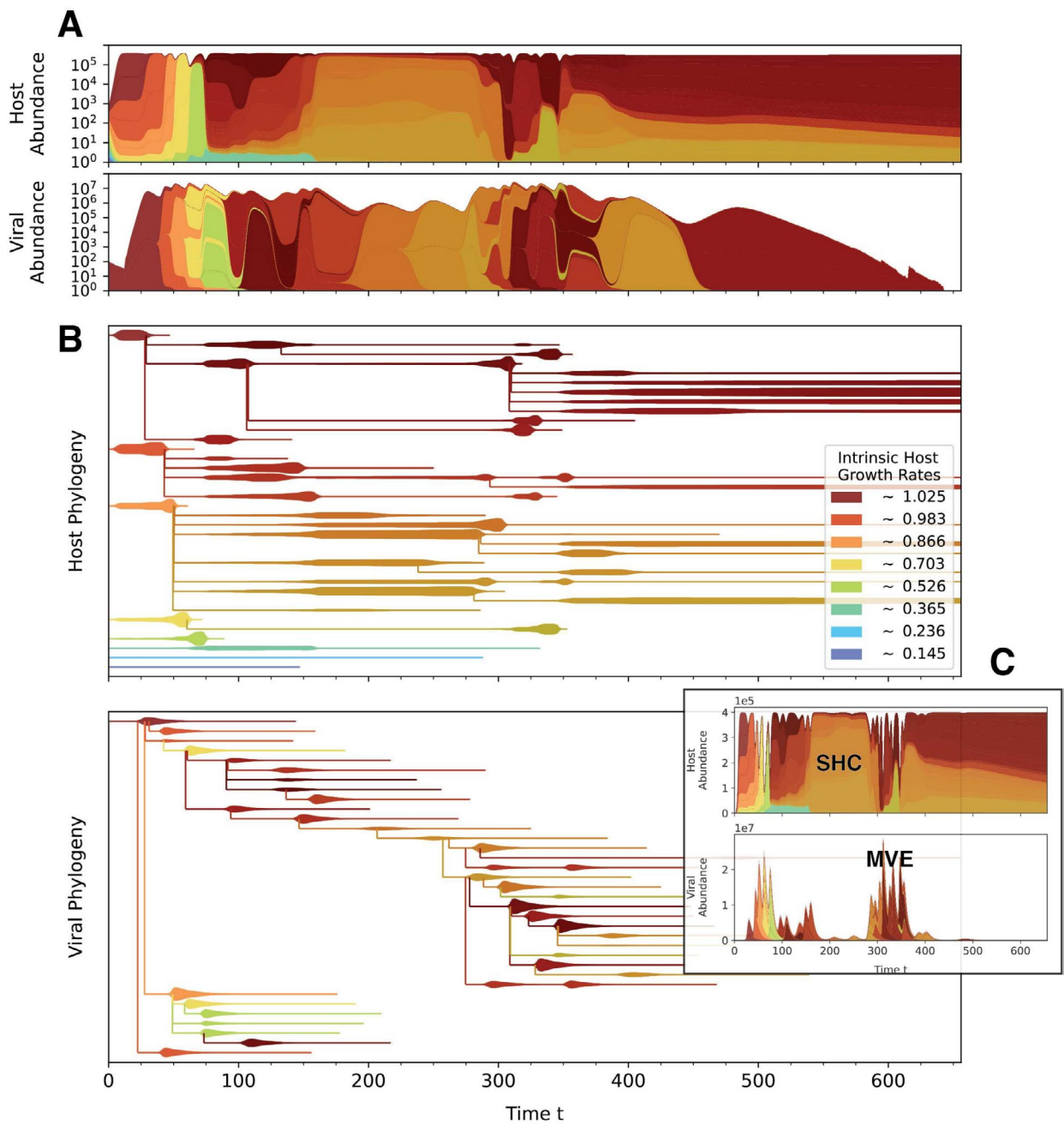


**FIGURE 2** | An example simulation of our CRISPR-induced microbe-lytic virus coevolutionary model at a host selection intensity of  $\sigma = 3$  in treatment I. In spite of initial declines due to a major viral epidemic, the most competitively advantaged host clades regain dominance and diversify the most. In this example, competitive-ability mutations do not occur. See Figure S1 for example simulation of Treatment II. (A) Muller plots of host and virus abundances where each stacked colour represents the abundance of a respective strain. Total abundances are scaled logarithmically, and distinct strain abundances are scaled linearly. Each hue represents a distinct host clade established by the initial competitors. Initial competitors are represented by a lighter shade of the hue, and its daughter strains are represented by the darker shade. The viral strains are coloured with the hue of the most abundant host strain that they infect throughout the entire simulation. (B) Forward phylogenies corresponding to (A) where the width of branches represent linearly scaled abundances of a respective strain. (C) Dynamics corresponding to (A) and (B) but represented with linear total abundances. Despite the inclusion of host competitive asymmetries, this model recapitulates the previously described *alternating* dynamics (Liaghate et al. 2024). The regime of sustained host control (SHC) is a transient period where the host biomass is saturated at, or near, carrying capacity. The major viral epidemics regime is the short-lived rapid succession of epidemics generated by multiple viral strains, where rapid co-diversification also takes place.

spacer into its genome. The distinct collection of spacers accrued in a microbial host's lifetime defines their immune type. The spacers confer protection from, and cause the decay of, future viruses that carry at least one matching protospacer. The

total fitness of a host strain is thus a function of both its intrinsic growth rate  $r$  and its spacer array (see Figure 1 for a schematic depiction). Furthermore, recent evidence suggests SNP mutations and INDELs (insertions/deletions) occurring upon

spacer acquisition (Guillemet et al. 2022; Barrangou et al. 2013). To investigate possible consequences of such genomic changes, we allow for host traits encoding competitive ability to mutate upon spacer acquisition with a probability  $\mu_s$ . In this scenario, the phenotype of the mutants is assumed to be independent of the parental phenotypes and is sampled uniformly from the trait interval  $x \in [-1, 1]$  (with discrete increments of 0.02 to reduce computational complexity). Most mutations are consequently deleterious, conferring growth rates lower than that of the parental phenotype. This can be interpreted as the cost of immunity acquisition (similar to the cost of resistance in previous gene-for-gene models (Frank 1993; Sasaki 2000)). We refer to such mutations as *competitive-ability mutations* hereafter. Moreover, with a probability of  $1 - q$  upon adsorption, a virus can successfully lyse a microbe and release a burst of  $\beta$  virion daughters, where the probability of having a mutated protospacer is  $\mu$ . Note that we do not assume any variation in the intrinsic demographic rates of the virus, nor any costs from escape mutations (pleiotropic effects). We also note that an infinite allele assumption for viral protospacer mutation is imposed: Every protospacer mutation introduces true allelic novelty to the viral population. Here, ‘infinite’ refers to the possible protospacer alleles, as opposed to possible protospacer loci. For corresponding stochastic reactions see [Supporting Information](#).

We initialize our simulations with a single viral strain and eight distinct host strains, both represented by 100 individuals. The host competitive trait is designated by coloured vertical lines in plot of its Gaussian growth function in Figure 1. For our primary treatment, *Treatment I*, we designate the host strain with the highest intrinsic growth rate to be completely susceptible to the single viral strain, whereas the other seven strains are chosen so that each has a distinct single-spacer match sampled at random from the  $g$  protospacer loci of a viral repertoire. Alongside, we also consider a second treatment, *treatment II*, comprising of eight host strains and eight viral strains. Each viral strain population can infect only one host strain population, where each host strain is protected from other viral strains with a single-spacer match. For Treatment II, we define the total viral population size to be  $\sim 100$ , where each viral strain population is a fraction thereof. Results pertaining to Treatment II, and competitive-ability mutations, are in the [Supporting Information](#).

### 3 | Results

#### 3.1 | Lineages of Host Strains With Highest Competitive Abilities Gain and Maintain Dominance, Representing the Majority of Immune Diversity

In this section, with numerical simulations of our stochastic model, we establish the long-term coevolutionary outcomes of diversity in both host adaptive immunity and intrinsic growth rates, emerging from the combined effect of negative frequency-dependent and directional selection. The Gaussian function of Figure 1 exemplifies the distribution of our initialized host strains for selection intensity  $\sigma = 3$  in Treatment I. Muller plots in (Figure 2A; see Figure S1 for example of treatment II) depict a realised example of host and virus population dynamics, including forward phylogenies (Figure 2B). Note that, similar

to the previous computational model of Liaghat et al. (Liaghat et al. 2024), the simulated dynamics exhibit transitions between a regime of sustained host control (SHC) and one of major viral epidemics (MVE). In the SHC regime, the host population is near carrying capacity and small intermittent outbreaks occur. These small outbreaks progressively disassemble the immune structure of the host population, thus giving way to a transition to the MVE regime, where rapid host–virus co-diversification occurs as evident in the phylogenies (see (Liaghat et al. 2024) for detailed analysis). Transitions between the SHC and MVE regimes are more clearly observed in Figure 2C, where dynamics are illustrated with linear abundances.

To examine the dominance of the host clades established by the initial competitors, we track the expected mean of the host competitive abilities over time  $\mathbb{E}(\bar{r})$ . Here  $\bar{r}$  is the mean intrinsic growth rate in a single replicate, and  $\mathbb{E}(\bar{r})$  is the expectation of the mean  $\bar{r}$  among the 400 simulated replicates. As expected in the absence of viruses, we find that host strains with higher competitive advantages consistently out-compete other strains, causing the mean competitive ability of the host population to gradually converge to the maximal intrinsic growth rate of 1.025 (Figure 3A). However, when viruses are introduced, a rapid decline in the mean competitive ability of the host strains is expected to occur due to a large viral epidemic. Following the rapid initial decline, the mean competitive ability of the host population rebounds to a large value comparable to that of the host population when viruses are absent. For Treatment II, Figure S2B shows similar rebounding dynamics when a diverse set of viral strains are introduced. These observations are in contrast to KTW models where the dominance of competitors with different intrinsic growth rates cyclically alternate (i.e., fluctuating selection) (Thingstad 2000; Winter et al. 2010; Xue and Goldenfeld 2017). Note that the observed resurgence of the dominant competitors remains robust in the case of competitive-ability mutations (Figure S2A; see also Treatment II in Figure S2C).

When the virus is absent, the Simpson index of immune diversity in both treatments gradually declines as expected, due to the competitive exclusion of host strains (Figure 3B). The Simpson index is given here by  $1 / \sum_i^S n_i^2$  where  $n_i$  is the frequency of a host immune strain with a unique spacer array  $i$ , and  $S$  is the total number of host immune strains. When the virus is present, this index declines upon the first expected viral epidemic for both Treatments I and II. The host phylogenies of Figure 2 and Figure S1 suggest that this decline of Simpson diversity is accompanied by viral outbreaks that tend to preferentially consume host strains with higher intrinsic growth rates before those with lower intrinsic growth rates. Due to the density dependence of infections, competitively advantaged host strains which tend to represent larger proportions of the carrying capacity are more likely to be infected than co-occurring competing strains. Upon the termination of the major viral epidemics, the Simpson index rebounds and surpasses levels of the initial period. This rebound of immune diversity is not due to a recovery of the older diversity, but rather to the nonstationary, cumulative diversification of the host clades. This is demonstrated by the increase in immune richness after the first few viral epidemics in Figure 3C. Richness here refers to the number of unique spacer arrays

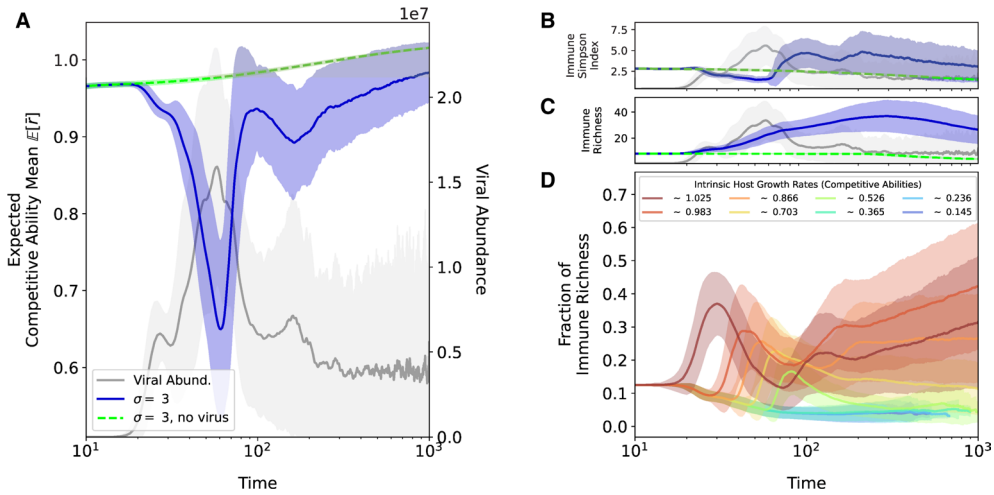


**FIGURE 3** | Host diversity expectations computed for a given regime of host selection ( $\sigma = 3$ ), with and without the viral population (blue and green curves, respectively) in Treatment I. Expected total viral abundance is represented by the grey curves. Light shades represent the standard deviation among the 400 simulated replicates. (A) The expected competitive ability for the host population over time. ‘Competitive ability’ specifically refers here to the intrinsic growth rates of the host strains.  $\bar{r}$  is the mean intrinsic growth rate in a single replicate, and  $E(\bar{r})$  is the expectation of the mean  $\bar{r}$  among the 400 simulated replicates. The lighter blue shade represents the standard deviation among replicates, and not within a single replicate. Despite the rapid initial rapid decline of the fittest host strains due to a viral epidemic, the fittest host strains rebound back into dominance. (B) The expected Simpson index of the host immune strains over time. Upon the first expected viral epidemic, the Simpson diversity rapidly drops. Thereafter, the Simpson diversity surpasses values of the initial period. (C) The dynamics of immune strain richness show that the increase in Simpson diversity is not due to the recovery of older diversity, but rather to the nonstationary diversification that occurs upon immune acquisition. (D) The proportion of total immune strain richness represented by the clades established by the initial competitors. The three clades with highest intrinsic growth rates diversify the most on average, and thus represent the majority of the immune diversity in the population after the first major viral epidemic.

in the host population. Note that increases in richness reflect true accumulation of immune diversity, unlike rises in the Simpson index which indicate compositional shifts.

Figure 3D shows the fraction of the immune richness represented by the clades established by the initial competitors. The clades originating from competitively dominant hosts, that is, those with the highest intrinsic growth rates, diversify the most on average. For our instantiation of host intrinsic growth rates, after the first few viral epidemics, the majority of the immune diversity is represented by three clades with the highest intrinsic growth rates (1.025,  $\sim .983$  and  $\sim .866$  in Figure 3D, despite the initial collapse due to viral infections. Consequently, the majority of immune diversity generated from past coevolution is largely represented by clades established by the initially competitively dominant host strains. The phylogeny and Muller plot of the host strains in Figure 2 demonstrate an example of how the majority of immune diversification is associated the three most competitive clades. In the case of competitive-ability mutations, the immune diversity is represented by a more even distribution of the different host clades Figure S2A,C). This indicates that the resurgent competitors do not necessarily belong to the clades established by the initially dominant competitors.

### 3.2 | Expected Time to Ultimate Viral Extinction Increases With Asymmetries of Host Competition

To systematically examine the effect of host selection on viral persistence, we implement a parameter sweep for our model across a range of host selection intensities for both Treatments I

and II. For each of the treatments, we also consider varied probabilities of competitive-ability mutations. For a geometrically incremented set of host selection intensities ( $\sigma \in [0, 10]$ ), we simulate 400 realisations of the microbe–virus coevolutionary dynamics. Namely, at one extreme is the regime of no host selection ( $\sigma = 0$ ), where host strains are competitively equivalent (neutral) and thus have equal intrinsic growth rates, whereas at the other extreme is the regime of strong host selection ( $\sigma = 10$ ) where competition is strongly asymmetric and introduces variation in the intrinsic growth rates. For each realisation, we compute the time to ultimate viral extinction, as well as associated quantities including the number of MVEs, the duration of SHC periods that separate MVEs, the mean number of viral mutants generated and spacers acquired per outbreak.

For our selected parameter values, the viral population eventually goes to extinction. This is a common outcome of CRISPR-mediated coevolution in previous computational models (Pilosof et al. 2020; Liaghat et al. 2024), also observed in experimental studies (Common et al. 2019, 2020; Paez-Espino et al. 2015). Figure 4A shows that the ultimate viral extinction times exhibit an increasing trend as host selection intensifies, for Treatment I in the absence of competitive-ability mutations. A Kruskal–Wallis  $H$ -test for the trend supports a significant increasing shift in the medians of extinction times at the higher selection intensities ( $p$  value of  $\sim 6.03 \cdot 10^{-68}$ , see [Supporting Information](#) for more details). In correspondence to the increasing trend of extinction times, viral evolution tends to accelerate as a function of host selection intensity. Namely, the viral population more frequently and rapidly overcomes SHC periods, thus generating more MVEs (Figure 4B,C).

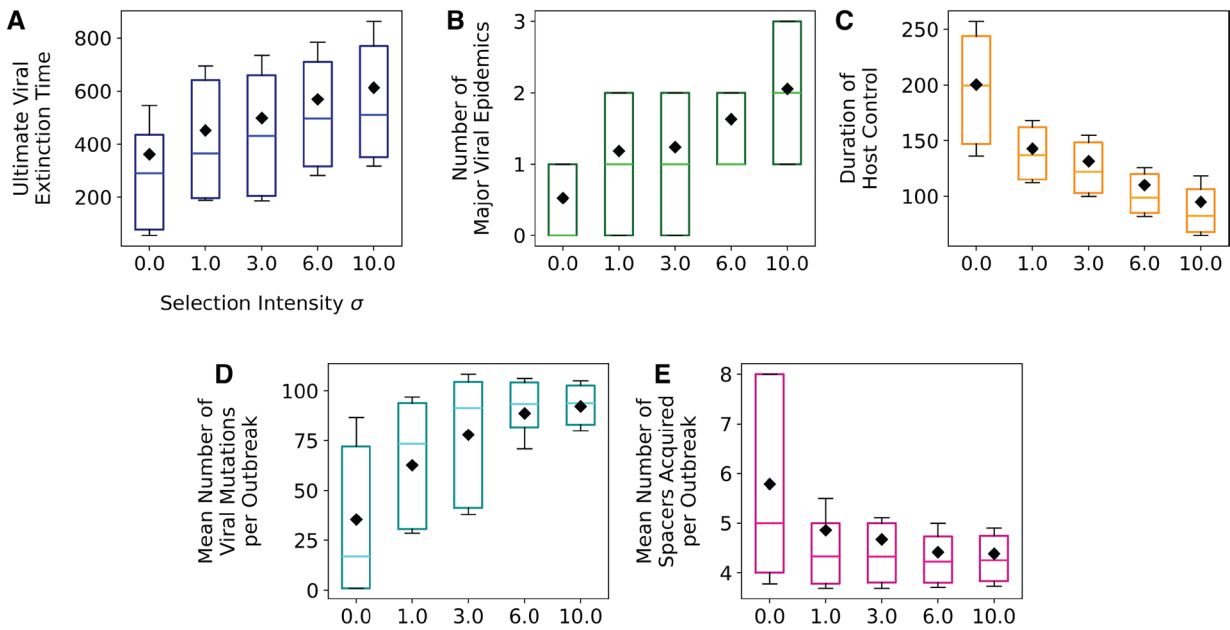


**FIGURE 4** | Box-and-whisker plots capture distributions of the time to ultimate viral extinction, and associated metrics, as a function of host selection intensity  $\sigma$  in Treatment I. The interquartile ranges represent 20%–80% of the simulated replicates. The black diamonds represent mean values, and the coloured horizontal lines in the interquartile ranges represent medians. (A) As host selection intensifies, times to ultimate viral extinction tend to increase ( $p \sim 6.03 \cdot 10^{-68}$  from a Kruskal–Wallis  $H$ -test), (B) major viral epidemics also become more frequent. (C) The duration of host control, which transiently separate these major viral epidemics, also shortens. This pattern suggests rapid disassembly of host immune structure. (D) The mean number of viral mutants per outbreak also tends to increase as host selection intensifies, whereas the mean number of spacers acquired per outbreak decreases (E). This suggests that recurrent viral escapes are more likely as host selection intensifies. See Figure S3 for emergent trends in the context of competitive-ability mutations, and Figure S4 for treatment II.

Note that we designate a major viral epidemic as one that causes a large decline of the host population (of *at least* 45%). Furthermore, as host selection intensifies, the mean number of viral mutants generated per outbreak increases, whereas the mean number of spacers acquired per outbreak decreases (Figure 4D,E). This suggests that a decline in host immune diversity, driven by strong directional selection, facilitates a disproportionate increase in viral density and thus diversity. Such viral diversification increases the likelihood of escapes from host immunity. In the case of Treatment II, similar to Treatment I, an increasing trend of time to ultimate viral extinction is observed as host selection intensifies. Increasing and decreasing trends for the number of MVEs and duration of SHC periods, respectively, are also observed. However, in contrast to Treatment I, the trends appear to converge as host selection intensifies and exhibit larger variance (Figure S4A). This may be an effect induced by the drift of viral strain populations. Each viral strain population in Treatment II is represented by a small fraction of 100 individuals (Section 2), and consequently is subject to more stochasticity than a single viral strain population in Treatment I. The emergence of an epidemic by a given viral strain is therefore less likely in Treatment II, than in Treatment I. An extensive exploration of the effect of inocula sizes, and its associated stochasticity, is outside the scope of this work and remains for future studies.

Moreover, the increasing trend in viral extinction time is lost as competitive-ability mutations become more probable in both Treatments I and II (Figures S3.1, S4.1). Despite this weakening of the trend, viral evolution tends to accelerate as host selection intensifies. This is demonstrated by the increase in MVEs and

shortening of SHC durations as host selection intensifies, which also become concentrated into the earlier times of the dynamics (Figures S3.3–5, S4.3–5). In addition, viral diversification is generally greater in the presence of competitive-ability mutations than in their absence (Figures S3.6, S4.6). In spite of this, as competitive-ability mutations become more probable, the mean number of spacers acquired per outbreak reveals an increasing trend as a function of host selection intensity (Figures S3.7 and S4.7). This is in contrast to the decreasing trend observed in the absence of competitive-ability mutations (Figure 4D), suggesting that with the acceleration of viral evolution, host immune evolution also accelerates, promoting the rapid assembly of immune structure needed to extinguish the viral population.

During periods of sustained host control, a viral strain consumes virtually all of its pool of susceptible host strains upon a small outbreak (Liagh et al. 2024). Therefore, in order for the total viral population to adapt and further persist, a viral strain must escape competing host strains upon an outbreak. To obtain a closer look at the effect of host selection on viral escape over time, we next consider two summary quantities often used to investigate coevolutionary dynamics, namely temporal and local adaptation.

### 3.3 | Strong Competitive Asymmetries of Host Population Promote Viral Evolution and Adaptation

Each viral escape permits access to a new pool of susceptible host strains, which increases the fitness of the total viral population. This effect on viral fitness, however, is only transient, as

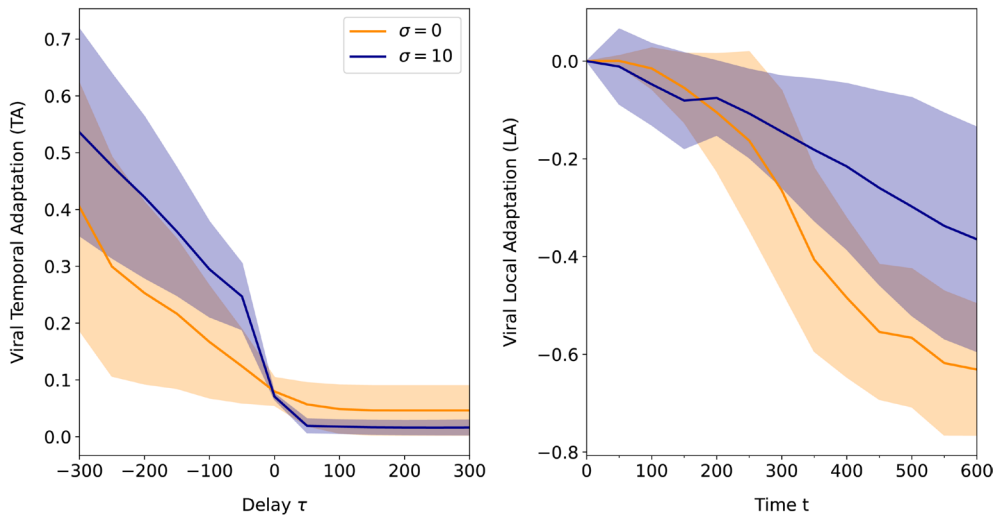


**FIGURE 5** | Temporal adaptation (TA) and local adaptation (LA) measures of the viral population for both extrema of host selection intensity ( $\sigma = 0$  and  $\sigma = 10$ ). The temporal adaptation quantity captures on average how adapted the viral population is to the host population from a retarded or advanced time shift of  $\tau$ . The local adaptation quantity determines whether the virus is on average more adapted to sympatric (same replicate) than to allopatric (different replicate) host populations. Here viral adaptation refers to the mean viral fitness, that is, mean frequency of susceptible hosts per viral strain. See Equations S1 and S2 for more details. Note that  $TA = 1$  indicates that the viral population is on average completely adapted to the host population of a time shift  $\tau$ , and  $TA = 0$  indicates the viral population is completely maladapted. Also note that  $LA = 1$  indicates that the viral population is completely sympatrically adapted but not allopatrically adapted, whereas  $LA = -1$  indicates the reverse. TA demonstrates a declining trend for both selection intensities, which indicates the propensity for viral maladaptation. Both TA and LA rapidly drop for both extrema of host selection intensity. However, in the absence of host selection, viral maladaptation is more rapid than for strong selection.

the viral population tends to *burn* through its pool of susceptible host strains (see (Liaghat et al. 2024)). If the viral population can generate another escape variant upon an outbreak, the total viral population can regain fitness and persist for another duration of time. Along with viral escapes, the host can acquire spacers upon an outbreak. This acquired immunity also tends to accumulate during host control periods. The long-term persistence of the viral population is thus contingent on its ability to recurrently escape acquired immunity and consequently generate outbreaks (Liaghat et al. 2024). Figure 4 suggests that host selection intensity must then modulate these recurrent and temporally localised gains and losses of viral fitness.

We examine changes of viral fitness more closely in the context of different host selection intensities, with measures of viral temporal adaptation (TA) and local adaptation (LA). Both quantities are functions of mean viral fitness  $\bar{\omega}$  (Supporting Information). The temporal adaptation quantity in Equation S7 captures on average how adapted the viral population is to the host population from a retarded or advanced time shift of  $\tau$ . This quantity can be used in empirical or experimental settings to identify the type of selection occurring in a coevolutionary system (Gandon et al. 2008; Blanquart and Gandon 2013). The local adaptation quantity in Equation S8 determines whether the virus is, on average, more adapted to sympatric (same replicate) than to allopatric (different replicate) host populations. See Equations S7 and S8 in Supporting Information for full expressions of TA and LA.

We observe that viral TA to the host population is maximal in the recent past, and exhibits a decreasing trend, for both extrema of host selection intensity:  $\sigma = 0$  and  $\sigma = 10$  (see Figure 5 and Figure S5 for Treatments I and II, respectively). This decreasing

trend reflects that the viral population overcomes accumulated host immunity through recurrent escapes throughout the dynamics. In contrast, viral TA rapidly drops when matched against hosts from the future. This demonstrates how rapidly hosts are able to acquire spacers, and thus immunity, from dominant viral strain. Furthermore, in the context of strong host selection, viral TA in the recent past is steeper in slope than in the absence of host selection. This corresponds to the acceleration of viral evolution suggested by the previous trends of the number of major viral epidemics, the durations of the SHC period in between, and their times of occurrence (Figure 4, Figures S3 and S4). The observed form of viral TA also suggests ‘arms-race’ frequency dynamics of viral diversity (Gandon et al. 2008; Blanquart and Gandon 2013). The augmented slope in the recent past is also observed in the context of competitive-ability mutations. Despite the detrimental effect of competitive-ability mutations on viral persistence, this result is consistent with the observed acceleration of viral evolution observed in Figures S3 and S4.

Lastly, we observe that viral local adaptation (LA) rapidly declines for both cases of host selection intensity (Figure 5 and Figure S6 for Treatments I and II, respectively). In particular, we observe that LA declines more slowly in a regime of strong host selection intensity, regardless of competitive-ability mutations (Figure S6). This implies that, on average, the viral population evolves to be more sympatrically adapted in the context of strong host selection than in the absence of host selection. Interestingly, local mean viral fitness for both cases of selection is expected to remain relatively constant, and of comparable values, throughout the dynamics (Figure S7). The mean viral fitness among contemporaneous, allopatric host populations is thus the main driver of the observed differences in LA in the two cases of host

selection. Namely, allopatric adaptation is more rapid in the absence of host selection.

## 4 | Discussion

By including host competitive asymmetries in a previous stochastic model of CRISPR-induced microbe-lytic virus coevolution, we are able to gain insight into the effects of two co-occurring modes of selection on viral evolution. These modes correspond respectively to negative frequency-dependent selection arising from immune microbial memory and directional selection from host competitive asymmetries. Following an initial major decline in host abundance due to a viral epidemic, competitively advantaged host strains rebound to maintain dominance in the population, representing the majority of immune diversity generated throughout the coevolutionary dynamics. As host selection intensifies, the time to ultimate viral extinction increases, which is also associated with the acceleration of viral evolution. Temporal and local adaptation measures also document short- and long-term behaviours of viral (mal-)adaptation in the two extreme regimes of host selection.

Our numerical results in conjunction with previous experimental work (Guillemet et al. 2022), support the recent ‘royal family’ hypothesis (Breitbart et al. 2018), which posits that newly rising host genotypes are likely to descend from previous genotypes that are dominant due to intrinsic asymmetries in competitive abilities. In ‘royal family’ dynamics, host strains with competitive advantages maintain dominance despite viral predation. This is in contrast to ‘kill-the-winner’ dynamics, where the preferential targeting of host strains with competitive differences, by the viral populations, alternates between those with high and low competitive advantages. Each host strain thus undergoes cycles of high and low frequencies, reflecting fluctuating selection (Thingstad 2000; Winter et al. 2010; Xue and Goldenfeld 2017; Marantos et al. 2022). Specificity in such preferential targeting would apply to surface resistance and restriction modification systems. It remains an open question whether these two different types of frequency-dependent dynamics arise due to memory operating at different organisational levels: both the individual and population level for CRISPR-induced immunity in royal family, and solely the population level for kill-the-winner. Also, despite the frequent co-occurrence of these differing lines of viral defence mechanisms in natural microbial populations, theoretical expectations of resulting eco-evolutionary dynamics are sparse and remain open for future research (for examples of multidefence in general host-parasite systems, see (Shudo and Iwasa 2001; Hamilton et al. 2008)). Furthermore, ‘royal’ viral lineages may also emerge due to competitive differences from variation in other demographic and interaction parameters in both microbes and viruses.

The observed trend of viral temporal adaption in our study is consistent with ‘arms-race’ frequency-dependent dynamics among viral strains (Gandon et al. 2008; Blanquart and Gandon 2013) and with viral temporal adaptation signatures in both the monomorphic and polymorphic experimental treatments of Guillemet et al. (Guillemet et al. 2022). The characteristic punctuated nature of viral and host diversification in ‘arms race’ dynamics, and its associated periods of explosive diversification, are so far

unique to CRISPR-mediated coevolution. Moreover, viral local adaptation demonstrates a declining trend over time for both of our Treatments I and II. In the monomorphic treatments of Guillemet et al., a partial decline may be observed as the experiments terminate, but the significance of this decline remains inconclusive. Our model assumes ‘infinite protospacer alleles’ (Methods), where every mutation introduces a novel protospacer allele among the  $g$  protospacer loci that define a viral strain. It therefore applies to the scenario of rapid loss of deleterious protospacer alleles occurring from back-mutations. The resulting trend of viral local adaptation captures potential long-term coevolutionary behaviour of empirical systems. In contrast, the experiments of Guillemet et al. capture short-term coevolutionary behaviour. Future experiments examining the long-term behaviour of CRISPR-mediated coevolutionary dynamics, will aid in further corroboration of our theoretical expectations. In addition, molecular experiments examining the probability of protospacer back-mutations will help refine how viral diversification is modelled.

Our results indicate that host competitive asymmetries can facilitate viral escape, thus delaying total viral extinction. When immunity carries costs via competitive-ability mutations, the same asymmetries reverse this effect, precipitating faster viral extinction even as they accelerate viral evolution and promote their diversity. This increase in viral diversity aligns with previous gene-for-gene models predicting broader pathogen diversity as host resistance costs rise (Frank 1993; Sasaki 2000). However, we also observe that host spacer repertoires diversify more strongly with increasing asymmetry under costly immunity, a pattern that merits further investigation in future studies. Nevertheless, across both cost regimes, our simulations frequently trend toward complete viral extinction and thus transient coevolution, also observed in previous computational and experimental studies (Childs et al. 2012; Pilosof et al. 2020; Liaghat et al. 2024; Common et al. 2019, 2020; Paez-Espino et al. 2015). Yet in natural microbe-virus communities, lytic viruses persist and the trailer-end spacers of host CRISPR-Cas arrays appear conserved for approximately 5 years or longer (Weinberger et al. 2012; Sun et al. 2016). The question of viral persistence thus requires further consideration. Initial conditions such as viral inocula sizes upon community assembly is one such direction; a metapopulation context is another. Notably, the measure of viral local adaptation in this study reveals strong allopatric adaptation, suggesting that viral emigration to foreign localities may indeed prolong viral persistence. Another future direction is the explicit consideration of resource dynamics and associated variation in consumer preferences in multitrophic systems, as our model implicitly captured the variation associated with consumption preferences and their corresponding rates.

The role of counteracting selective forces—arising from distinct trait axes—in shaping community dynamics and diversity has long been recognised in ecological theory, particularly within the framework of Modern Coexistence Theory (e.g., (Chesson 2000)). Some models have incorporated such a framework of opposing modes of selection in the coevolutionary context, including multilocus gene-for-gene frameworks with resistance-associated fitness costs (Frank 1993; Sasaki 2000), and a recent eco-evolutionary consumer-resource model that

captures the relationship between resource strategies and utilisation efficiencies (Good et al. 2018). While such approaches offer valuable theoretical insights, they are ill-equipped to represent the high-dimensional trait architectures increasingly revealed by microbial pangenomics. This underscores the need to explicitly integrate high-dimensional trait specificity as well as ecological feedbacks and demography into coevolutionary theory. Doing so would bridge the gap between theory and empirical data and lay the groundwork for a more comprehensive synthesis of coevolutionary dynamics, which remains missing to date.

A formal synthesis of coevolutionary dynamics that accounts for multidimensional traits and specificity would enable clearer expectations for both the structural and temporal patterns of co-evolving systems under distinct ecological scenarios. These insights would help clarify the specific conditions required for the emergence of previously hypothesised dynamics: canonical ones like Red Queen, arms-race, kill-the-winner and more recent ones like the royal family. Our study contributes to this broader synthesis by showing that host competitive asymmetries not only give rise to royal-family dynamics within the host population but also modulate the timescale of viral evolution driven by negative frequency-dependent selection.

## Author Contributions

A.L., M.G., R.W., S.G. and M.P. conceived the study. A.L. implemented numerical simulations of the model and conducted the mathematical and numerical analyses. A.L. wrote the manuscript. All authors contributed to editing and reviewing the final text.

## Acknowledgements

This work was supported by the Gordon and Betty Moore Foundation, GBMF 9195, and by the GEMS Biology Integration Institute, funded by the National Science Foundation DBI Biology Integration Institutes Programme, Award Number 2022049.

## Conflicts of Interest

The authors declare no conflicts of interest.

## Data Availability Statement

Codes for model, analyses and figures are publicly hosted by a GitHub repository: <https://github.com/pascualgroup/crispr-competitive-asymmetries>.

## Peer Review

The peer review history for this article is available at <https://www.webofscience.com/api/gateway/wos/peer-review/10.1111/ele.70153>.

## References

Allesina, S., and S. Tang. 2012. "Stability Criteria for Complex Ecosystems." *Nature* 483, no. 7388: 205–208.

Barabás, G., R. D'Andrea, and S. M. Stump. 2018. "Chesson's Coexistence Theory." *Ecological Monographs* 88, no. 3: 277–303.

Barrangou, R., A.-C. Coûté-Monvoisin, B. Stahl, et al. 2013. "Genomic Impact of Crispr Immunization Against Bacteriophages." *Biochemical Society Transactions* 41, no. 6: 1383–1391.

Blanquart, F., and S. Gandon. 2013. "Time-Shift Experiments and Patterns of Adaptation Across Time and Space." *Ecology Letters* 16, no. 1: 31–38.

Breitbart, M., C. Bonnain, K. Malki, and N. A. Sawaya. 2018. "Phage Puppet Masters of the Marine Microbial Realm." *Nature Microbiology* 3, no. 7: 754–766.

Chabas, H., S. Lion, A. Nicot, et al. 2018. "Evolutionary Emergence of Infectious Diseases in Heterogeneous Host Populations." *PLoS Biology* 16, no. 9: e2006738.

Chesson, P. 2000. "Mechanisms of Maintenance of Species Diversity." *Annual Review of Ecology and Systematics* 31, no. 1: 343–366.

Childs, L. M., W. E. England, M. J. Young, J. S. Weitz, and R. J. Whitaker. 2014. "Crispr-Induced Distributed Immunity in Microbial Populations." *PLoS One* 9, no. 7: e101710.

Childs, L. M., N. L. Held, M. J. Young, R. J. Whitaker, and J. S. Weitz. 2012. "Multiscale Model of Crispr-Induced Coevolutionary Dynamics: Diversification at the Interface of Lamarck and Darwin." *Evolution* 66, no. 7: 2015–2029.

Common, J., D. Morley, E. R. Westra, and S. van Houte. 2019. "Crispr-Cas Immunity Leads to a Coevolutionary Arms Race Between *Streptococcus Thermophilus* and Lytic Phage." *Philosophical Transactions of the Royal Society B* 374, no. 1772: 20180098.

Common, J., D. Walker-Sünderhauf, S. van Houte, and E. R. Westra. 2020. "Diversity in Crispr-Based Immunity Protects Susceptible Genotypes by Restricting Phage Spread and Evolution." *Journal of Evolutionary Biology* 33, no. 8: 1097–1108.

Doebeli, M., and I. Ispolatov. 2010. "Complexity and Diversity." *Science* 328, no. 5977: 494–497.

Frank, S. A. 1993. "Coevolutionary Genetics of Plants and Pathogens." *Evolutionary Ecology* 7: 45–75.

Gandon, S., A. Buckling, E. Decaestecker, and T. Day. 2008. "Host-Parasite Coevolution and Patterns of Adaptation Across Time and Space." *Journal of Evolutionary Biology* 21, no. 6: 1861–1866.

Good, B. H., S. Martis, and O. Hallatschek. 2018. "Adaptation Limits Ecological Diversification and Promotes Ecological Tinkering During the Competition for Substitutable Resources." *Proceedings of the National Academy of Sciences of the United States of America* 115, no. 44: E10407–E10416.

Guillemet, M., H. Chabas, A. Nicot, et al. 2022. "Competition and Coevolution Drive the Evolution and the Diversification of Crispr Immunity." *Nature Ecology & Evolution* 6, no. 10: 1480–1488.

Hamilton, R., M. Siva-Jothy, and M. Boots. 2008. "Two Arms Are Better Than One: Parasite Variation Leads to Combined Inducible and Constitutive Innate Immune Responses." *Proceedings of the Royal Society B: Biological Sciences* 275, no. 1637: 937–945.

Hyun, J. C., J. M. Monk, and B. O. Palsson. 2022. "Comparative Pangenomics: Analysis of 12 Microbial Pathogen Pangenomes Reveals Conserved Global Structures of Genetic and Functional Diversity." *BMC Genomics* 23, no. 1: 1–18.

Liaghat, A., J. Yang, R. Whitaker, and M. Pascual. 2024. "Punctuated Virus-Driven Succession Generates Dynamical Alternations in Crispr-Mediated Microbe-Virus Coevolution." *Journal of the Royal Society Interface* 21, no. 217: 20240195.

Marantos, A., N. Mitarai, and K. Sneppen. 2022. "From Kill the Winner to Eliminate the Winner in Open Phage-Bacteria Systems." *PLoS Computational Biology* 18, no. 8: e1010400.

May, R. M. 1972. "Will a Large Complex System Be Stable?" *Nature* 238, no. 5364: 413–414.

Medini, D., C. Donati, H. Tettelin, V. Massignani, and R. Rappuoli. 2005. "The Microbial Pan-Genome." *Current Opinion in Genetics & Development* 15, no. 6: 589–594.

Mira, A., A. B. Martín-Cuadrado, G. D'Auria, and F. Rodríguez-Valera. 2010. "The Bacterial Pan-Genome: A New Paradigm in Microbiology." *International Microbiology* 13, no. 2: 45–57.

Morley, D., J. M. Broniewski, E. R. Westra, A. Buckling, and S. van Houte. 2017. "Host Diversity Limits the Evolution of Parasite Local Adaptation." *Molecular Ecology* 26, no. 7: 1756–1763.

O'Dwyer, J. P. 2018. "Whence Lotka-Volterra? Conservation Laws and Integrable Systems in Ecology." *Theoretical Ecology* 11, no. 4: 441–452.

Paez-Espino, D., I. Sharon, W. Morovic, et al. 2015. "Crispr Immunity Drives Rapid Phage Genome Evolution in *Streptococcus thermophilus*." *MBio* 6, no. 2: 10–1128.

Park, S. W., S. Cobey, C. J. E. Metcalf, J. M. Levine, and B. T. Grenfell. 2024. "Predicting Pathogen Mutual Invasibility and Co-Circulation." *Science* 386, no. 6718: 175–179.

Pilosof, S., S. A. Alcalá-Corona, T. Wang, et al. 2020. "The Network Structure and Eco-Evolutionary Dynamics of Crispr-Induced Immune Diversification." *Nature Ecology & Evolution* 4, no. 12: 1650–1660.

Pilosof, S., M. A. Porter, M. Pascual, and S. Kéfi. 2017. "The Multilayer Nature of Ecological Networks." *Nature Ecology & Evolution* 1, no. 4: 0101.

Rouli, L., V. Merhej, P.-E. Fournier, and D. Raoult. 2015. "The Bacterial Pan-genome as a New Tool for Analysing Pathogenic Bacteria." *New Microbes New Infections* 7: 72–85.

Sasaki, A. 2000. "Host-Parasite Coevolution in a Multilocus Gene-For-Gene System." *Proceedings of the Royal Society of London. Series B: Biological Sciences* 267, no. 1458: 2183–2188.

Shudo, E., and Y. Iwasa. 2001. "Inducible Defense Against Pathogens and Parasites: Optimal Choice Among Multiple Options." *Journal of Theoretical Biology* 209, no. 2: 233–247.

Song, C., G. Barabás, and S. Saavedra. 2019. "On the Consequences of the Interdependence of Stabilizing and Equalizing Mechanisms." *American Naturalist* 194, no. 5: 627–639.

Sun, C. L., B. C. Thomas, R. Barrangou, and J. F. Banfield. 2016. "Metagenomic Reconstructions of Bacterial Crispr Loci Constrain Population Histories." *ISME Journal* 10, no. 4: 858–870.

Thingstad, T. F. 2000. "Elements of a Theory for the Mechanisms Controlling Abundance, Diversity, and Biogeochemical Role of Lytic Bacterial Viruses in Aquatic Systems." *Limnology and Oceanography* 45, no. 6: 1320–1328.

Thrall, P. H., and J. J. Burdon. 2003. "Evolution of Virulence in a Plant Host-Pathogen Metapopulation." *Science* 299, no. 5613: 1735–1737.

Van Der Oost, J., E. R. Westra, R. N. Jackson, and B. Wiedenheft. 2014. "Unravelling the Structural and Mechanistic Basis of Crispr-Cas Systems." *Nature Reviews Microbiology* 12, no. 7: 479–492.

van Houte, S., A. K. Ekroth, J. M. Broniewski, et al. 2016. "The Diversity-Generating Benefits of a Prokaryotic Adaptive Immune System." *Nature* 532, no. 7599: 385–388.

Weinberger, A. D., C. L. Sun, M. M. Pluciński, et al. 2012. "Persisting Viral Sequences Shape Microbial Crispr-Based Immunity." *PLoS Computational Biology* 8, no. 4: e1002475.

Winter, C., T. Bouvier, M. G. Weinbauer, and T. F. Thingstad. 2010. "Trade-Offs Between Competition and Defense Specialists Among Unicellular Planktonic Organisms: The "Killing the Winner" Hypothesis Revisited." *Microbiology and Molecular Biology Reviews* 74, no. 1: 42–57.

Xue, C., and N. Goldenfeld. 2017. "Coevolution Maintains Diversity in the Stochastic "Kill the Winner" Model." *Physical Review Letters* 119, no. 26: 268101.

## Supporting Information

Additional supporting information can be found online in the Supporting Information section.